Technical Report TUBS-CG-1998-01

Dithered Color Quantization

J. M. Buhmann[1], Dieter W. Fellner, M. Held[1], J. Ketterer[1], J. Puzicha[1]
{d.fellner}@tu-bs.de

Institute of Computer Graphics
University of Technology
Mühlenpfordtstr. 23, D-38106 Braunschweig
http://graphics.tu-bs.de

[1]University of Bonn, Germany

EUROGRAPHICS '98 / N. Ferreira and M. Göbel
(Guest Editors)

Volume 17, (*1998*), *Number 3*

Dithered Color Quantization

J.M. Buhmann,* D.W. Fellner,** M. Held,* J. Ketterer,* and J. Puzicha* †

Departments of Computer Science, University of Bonn* and TU Braunschweig,** Germany

Abstract

Image quantization and digital halftoning are fundamental problems in computer graphics, which arise when displaying high-color images on non-truecolor devices. Both steps are generally performed sequentially and, in most cases, independent of each other. Color quantization with a pixel-wise defined distortion measure and the dithering process with its local neighborhood optimize different quality criteria or, frequently, follow a heuristic without reference to any quality measure.

In this paper we propose a new method to simultaneously *quantize and dither color images. The method is based on a rigorous cost–function approach which optimizes a quality criterion derived from a generic model of human perception. A highly efficient algorithm for* optimization *based on a multiscale method is developed for the dithered color quantization cost function. The quality criterion and the optimization algorithms are evaluated on a representative set of artificial and real–world images as well as on a collection of icons. A significant image quality improvement is observed compared to standard color reduction approaches.*

1. Introduction

True color images usually contain up to 16 million different colors. One of the basic tasks of computer graphics consists of reducing the number of colors with minimal visual distortion. Such a coarse graining of colors is of crucial importance, because many image display and printing devices provide only a limited number of colors. The representation problem for colors aggravates when many images are displayed simultaneously resulting in a palette size of 256 or even substantially less colors assigned to each image. Furthermore, fast image manipulation, image coding and image processing tasks often rely on operating on a reduced *color palette*.

Numerous techniques have been proposed for image quantization, most of which obey a two–step scheme:

1. Initially, a color set is selected by minimizing some pixel distortion error. Examples are the popular median–cut quantizer[1], octree quantization[2] and the application of a variety of clustering methods like LBG[3, 4] or self–organizing networks[5]. In fact, any suitable clustering approach could be used[6]. Characteristic for all clustering approaches is the fact that they neglect spatial, i.e. contextual, information.
2. Several types of degradation appear in the quantized image due to the limited number of colors, the most severe being the appearance of contouring artifacts in uniform regions. *Dithering* and *digital halftoning methods*[7] as a subsequent processing step address this problem by exploiting the low-pass filtering property of the human visual system. Human beings perceive high frequency variations in color as a *uniform* color. Impressionistic painters from the French school of pointillism have exploited this effect in a spectacular way as illustrated in Fig. 1. Therefore, additional illusory colors can be created by spatial mixing. In a common dithering technique called *error diffusion* the quantization error is spread to neighboring pixels, i.e. the distortion at neighboring pixels is biased in opposite direction. Several error diffusion filters have been proposed[7, 8]. In addition, *model–based halftoning*[9, 10, 11] techniques have been developed, which model human perception in more detail.

Quantization and dithering are generally performed sequentially[1, 2, 12, 13]. It is a key observation that quantization

† This work has been supported by the German Research Foundation (DFG) under grants Bu 914/3–1 and Fe 431/4–1, by the German Israel Foundation for Science and Research Development (GIF) under grant 1-0403-001.06/95 and by the Federal Ministry for Education, Science and Technology (BMBF 01 M 3021 A/4).

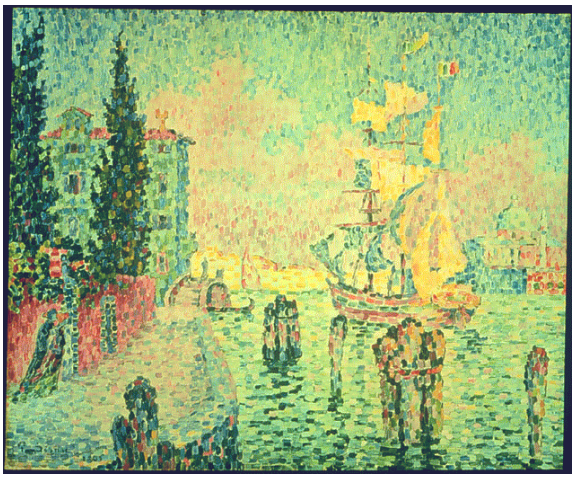

Figure 1: *Pointillism artwork by Paul Signac: 'La maison verte, Venice', 1905.*

and dithering procedures optimize different quality criteria. While clustering distortion criteria like the well–known K–means cost function are exclusively pixel–based, dithering techniques rely on spatial information and distribute the distortion error among neighboring pixels. While the necessity for combining both steps has been noticed before[12] joint quantization and dithering approaches have been considered only recently on a heuristic ad–hoc basis[14, 15].

In this paper we propose a rigorous cost–function based approach, which simultaneously performs quantization and dithering of color images in a joint error-minimizing algorithm, which we refer to as *dithered quantization*. The presented cost function extends the K–means criterion to a spatially weighted distortion measure. The cost function is based on a model of human color perception and can be understood as the Euclidean distance between the *perceived images* before and after quantization. It therefore incorporates dithering techniques into the quantization cost–function. The strengths of both, quantization and dithering, are combined in a rigorous fashion leading to a significant improvement in image display quality. The cost function is generic in the sense that the algorithms are developed independent of the specific details of the chosen perception model. A broad range of possible models of human color perception are covered[16, 17, 18, 19, 9, 10, 11]. From our point of view a successful optimization approach consists of two, conceptually well–separated parts:

1. A quality criterion, which appropriately *models* the information processing task: In the case of color reduction the global minima of the cost function should correspond to psychophysically pleasing image reproductions.
2. An efficient optimization algorithm to minimize the proposed cost function.

We develop a highly efficient optimization algorithm for the spatial clustering criterion, which is based on the **I**terative **C**onditional **M**ode (ICM) algorithm and which is similar in spirit to the well–known K–means clustering algorithm. The algorithm is iterative in nature, assigning image pixels to prototypical colors keeping the color palette fixed and than determining a new optimal color palette based on the current fixed assignments. This two step scheme is repeated until a minimum is reached. It is worth to point out again that, in contrast to traditional approaches, both steps minimize the identical error criterion. The two step iteration is an algorithmic implementation of the estimates of a color palette and the respective color assignments to pixels, but is not at all conceptually related to the two step procedure of quantization and dithering in conventional color reduction schemes.

The basic ICM is significantly accelerated by applying *multiscale optimization* techniques[20]. Multiscale optimization can be understood as the minimization of the original cost function over a properly reduced search space and has been shown to substantially speed up optimization algorithms for other clustering cost functions[21]. For dithered quantization the corresponding cost functions on coarse image grids are derived. In addition, the special local structure of the novel cost function enables adaptive site visitation schedules and the use of an efficient bookkeeping scheme yielding an acceptable overall time complexity of the proposed algorithms.

In Sect. 2 we discuss color spaces and present the novel dithered color quantization cost function. Sect. 3 is dedicated to optimization methods. Multiscale expressions are derived and the optimization algorithm is discussed in detail. Results are presented in Sect. 4 followed by a short conclusion.

2. Combining Quantization and Dithering

2.1. Perception model

It is well known that the capabilities of the human visual system drop rapidly approaching high spatial frequencies. This is due to the finite resolution of the human eye and the physical limitations of display devices. Thus, additional imaginary colors can be generated by *digital halftoning* since only a spatial average of the micro–variations are perceived. This has been exploited in a broad variety of error diffusion[8, 7], dithering[12] and model–based halftoning[9, 10, 11] applications to enhance the quality of quantized color images.

To simplify the model of imaginary colors the chosen color space should represent perceived superposition of colors as linear superpositions. A color space with this property is called a *uniform color space*. The commonly used RGB color space and its linear derivates do not constitute uniform color spaces. In contrast, the CIE $L^*a^*b^*$ and CIE $L^*u^*v^*$ color spaces[22] represent differences in color by the Euclidean metric in a psychophysically meaningful way. In

addition, a linearization of $L^*a^*b^*$ around the white point has been suggested for digital halftoning[9]. It is well known that the uniformity assumption suffers from some minor defects[23]. The uniformity assumption for both $L^*a^*b^*$ and $L^*u^*v^*$ is based on color matching experiments conducted with relatively large color patches and has thus been ensured only for low spatial frequencies. To overcome this shortness, new non-Euclidean metrics were proposed. Despite these facts, in this paper RGB and CIE $L^*a^*b^*$ color spaces with the Euclidean metric are used for computational simplicity. In addition, there is empirical evidence that the artifacts which are induced by the reduction to only a few colors dominate the effects of a slightly non–linear colorspace.

Having defined a uniform color space U, we model human perception as a linear blurring operation, i.e. a convolution of the input image with a localized kernel. This model is motivated by the extreme convergence between retina and the visual cortex, where neighboring receptors project on one ganglion and groups of ganglions converge to single neurons in the visual cortex[24]. Thus a substantial spatial averaging is performed in the early stages of human vision. In a more system theoretic interpretation this models the perception process as a linear system. An early filter model of human perception based on empirical data has been proposed by Campbell[16]. Several more elaborated models with a focus on spatial frequency response for luminance[17, 18, 10] and chrominance[19] have been advocated in the sequel.

The main focus of this contribution is the development of a combined method for simultaneous quantization and dithering. We will therefore abstract from the specific perception model at hand and develop *generic algorithms* for a broad class of possible human perception models defined by linear filters W_k. The filters W_k are allowed to differ for different color coordinates k to account e.g. for the different sensitivity of the human visual system with respect to luminance and chrominance variations.

To obtain a formulation for a discrete image grid we introduce a neighborhood system $N_{i,k}$ defined as the spatial support of the filter kernel W_k and define k–dimensional weight vectors $\mathbf{w}_{ij}$ for neighborhood pixels as being proportional to $W_k(r(i,j))$

$$w_{ijk} \propto W_k(r(i,j)), \quad j \in N_{i,k} \tag{1}$$

and $w_{ijk} = 0$ for $j \notin N_{i,k}$. Here $r(i,j)$ denotes the relative spatial position of pixel j with respect to pixel i. Introduce the maximal neighborhood system $N_i = \bigcup_k N_{i,k}$ for notational convenience. The *perceived color* $\mathbf{c}_i \in U$ at location i for a given image is modeled as

$$\mathbf{c}_i(\mathbf{X}) = \sum_{j \in N_i} \mathbf{w}_{ij} \circ \mathbf{x}_j \tag{2}$$

where $\mathbf{x}_j \in U$ denotes the pixel value at location j, $\mathbf{X} \in \Omega = U^N$ denotes the original color image of size N in raster scan order and $\circ$ denotes the element–wise multiplication. In the experiments we used a very simple model with a Gaussian kernel of identical standard deviation σ for all channels as transfer function. The weights $\mathbf{w}_{ij}$ for neighborhood pixels were defined for all channels k

$$w_{ijk} \propto \exp\left(-\frac{D_{ij}}{\sigma^2}\right), \quad \sum_{j \in N_i} w_{ijk} = 1 \tag{3}$$

using Euclidean distances D_{ij} between pixel i and pixel j.

2.2. Dithered Quantization Cost Function

To define the dithered quantization cost function we first introduce a set or palette of quantized colors, which are denoted by a vector of prototype variables $\mathbf{Y} = (\mathbf{y}_\nu^t)_{\nu=1,\dots,K}$, $\mathbf{y}_\nu \in U \subset \mathbb{R}^3$, where U is again an appropriately defined uniform color space and the superscript t denotes the transpose of a vector. A quantization is then defined as an assignment of pixel colors $\mathbf{x}_i$ to prototypical colors $\mathbf{y}_\nu$, which is formalized by Boolean assignment variables $M_{i\nu} \in \{0,1\}$. $M_{i\nu} = 1(0)$ denotes whether the image site $\mathbf{x}_i$ is (is not) quantized to color $\mathbf{y}_\nu$. All assignments are summarized in terms of a Boolean assignment matrix $\mathbf{M} \in \mathcal{M}$, where

$$\mathcal{M} = \left\{ \mathbf{M} \in \{0,1\}^{N \times K} : \sum_{\nu=1}^{K} M_{i\nu} = 1,\ 1 \le i \le N \right\} \tag{4}$$

The quantized image is now formally obtained by $\mathbf{MY}$. As a cost function for faithful color reproduction we employ the distance between the perceived image before and after quantization, where the perceived color after quantization is $\mathbf{c}_i(\mathbf{MY})$. For a linear color space the Euclidean norm is the natural choice yielding costs

$$\mathcal{H}(\mathbf{M},\mathbf{Y}) = \sum_{i=1}^{N} \|\mathbf{c}_i(\mathbf{X}) - \mathbf{c}_i(\mathbf{MY})\|^2 \tag{5}$$

$$= \sum_{i=1}^{N} \left\| \left(\sum_{j \in N_i} \mathbf{w}_{ij} \circ \mathbf{x}_j \right) - \left(\sum_{j \in N_i} \sum_{\nu=1}^{K} M_{j\nu} \mathbf{w}_{ij} \circ \mathbf{y}_\nu \right) \right\|^2 \tag{6}$$

The task of dithered quantization is then defined as a search for a parameter set $(\mathbf{M},\mathbf{Y})$ which minimizes (5). The classical K–means cost function,

$$\mathcal{H}^{\mathrm{km}}(\mathbf{M},\mathbf{Y}) = \sum_{i=1}^{N} \sum_{\nu=1}^{K} M_{i\nu} \|\mathbf{x}_i - \mathbf{y}_\nu\|^2 \tag{7}$$

is obtained for $w_{ijk} = \delta_{ij}$ and can be understood as the special case of our model with a blur free perception model. Notice that it is possible to (partially) fix a set of prototypes, e.g. a set of available colors, and to optimize the assignments of pixels to colors alone. Therefore, this cost function provides also a method for digital halftoning of an image given a fixed color table. In contrast to error diffusion equation (5) allows only local compensation of quantization errors. This avoids visually disturbing defects like error–accumulation[12].

In contrast to the K–means cost function, which is linear with respect to discrete and continuous parameter set,

cost function (5) is quadratic. Thus the substantial increase in modeling quality for our color quantization approach is contrasted by an increase in computational costs. The reader should be aware at this point that changes in the model of human perception only result in a different cost function, when assuming a non–linear perception model like average luminance dependency of the transfer function[18]. Thus all possible linear perception models are covered by the cost function (5) and the following presentation is completely independent of our specific choice in (3).

Our generic model incorporates the possibility of a different weighting of color channels[9]. A weighting of channel k by a factor c_k is achieved simply by multiplying the filter coefficients w_{ijk} by $\sqrt{c_k}$. Note that the model is spatially isotropic and the filter coefficients have only to be stored once. An extension to non–isotropic models is straightforward. For example, the filter model for luminance perception might depend on the absolute luminance value[18]. Ideas from anisotropic diffusion could be incorporated by adapting the filter on the luminance gradient to avoid halftoning across object boundaries. Non–isotropic models are implemented by allowing filter coefficients which depend on the input image, $\mathbf{w}_{ij} = \mathbf{w}_{ij}(\mathbf{x})$. The reader should note though that (5) can no longer be interpreted as the Euclidean distance of the perceived image before and after quantization, as $\mathbf{c}_i(\mathbf{MY})$ now depends on the original image data.

Our generic model even covers extensions to the time domain, where spatial averaging is accompanied or replaced by temporal averaging[25]. The neighborhood $\tilde{N}$ has to be extended into the time domain and an appropriate filter has to be selected as a perceptual model for temporal averaging. The developed algorithms are then applicable without change.

The cost function (5) can be rewritten as a quadratic form in the assignment variables $\mathbf{M}$ and in the continuous variables $\mathbf{Y}$. For this purpose, we introduce a new, enlarged neighborhood

$$\tilde{N}_i = \{k \,|\, \exists j : j \in N_i \cap N_k\} \tag{8}$$

Use the constants

$$\begin{aligned} \mathbf{b}_{ij} &= \sum_{k \in N_i \cap N_j} \mathbf{w}_{ik} \circ \mathbf{w}_{jk}, \quad j \in \tilde{N}_i \\ \mathbf{a}_i &= -2 \sum_{j \in \tilde{N}_i} \mathbf{b}_{ij} \circ \mathbf{x}_j \end{aligned} \tag{9}$$

for notational convenience and note that $\mathbf{b}_{ij}$ is invariant to translation and rotation, i. e. depends only on D_{ij} for our specific perception model (3). For spatially non–isotropic models the $\mathbf{b}_{ij}$ depend on the image position i and have a storage complexity of $|\Omega||\tilde{N}|$, which may be prohibitively high especially for image sequences. An equivalent expression for (5) is given by

$$\begin{aligned} \mathcal{H}(\mathbf{M},\mathbf{Y}) &= \sum_{i=1}^{N} \sum_{j \in \tilde{N}_i} \sum_{\nu=1}^{K} \sum_{\alpha=1}^{K} M_{i\nu} M_{j\alpha} \mathbf{y}_\alpha^t \left(\mathbf{b}_{ij} \circ \mathbf{y}_\nu\right) \\ &\quad + \sum_{i=1}^{N} \sum_{\nu=1}^{K} M_{i\nu} \mathbf{a}_i^t \mathbf{y}_\nu \end{aligned} \tag{10}$$

which makes the quadratic nature of $\mathcal{H}$ explicit. The constant term $\sum_{i=1}^{N} \left(\sum_{j \in N_i} \mathbf{w}_{ij} \circ \mathbf{x}_j\right)^2$ without influence on either the assignments or the prototypes has been discarded.

3. Optimization for Dithered Quantization

3.1. Optimization of Assignments using ICM

A common way to optimize mixed combinatorial optimization problems such as $\mathcal{H}(\mathbf{M},\mathbf{Y})$ is by alternating a minimization scheme, i.e. to optimize the discrete parameters while keeping the continuous parameters fixed and subsequently optimize the continuous parameters for a fixed discrete set. This twofold optimization is iterated until a predefined convergence criterion is fulfilled.

For fixed $\mathbf{Y}$ the cost function $\mathcal{H}(\mathbf{M},\mathbf{Y}) = \mathcal{H}(\mathbf{M})$ expresses a purely combinatorial problem, which can be efficiently solved by the local Iterative Conditional Mode (ICM) algorithm. It is well–known though that ICM gets frequently stuck in local minima. A more accurate global optimization algorithm known as deterministic annealing has been developed in a companion paper[26]. Deterministic annealing algorithms yield results of superior quality and are applicable without further technical difficulties but they are slower than ICM optimization by an order of magnitude. Intuitively, the ICM proceeds as follows:

- Start with a proper initialization of assignments of pixels to prototypical colors. Typically, the assignments of the last iteration (from the overall alternating minimization scheme) are taken while for the first iteration a random assignment matrix is used.
- Iterate through the image until no more assignment variables change.
- For each image site, keep the assignment variables of all other image sites fixed. Compute for all ν the costs $g_{i\nu}$ for assigning this site to prototypical color ν. The so–called *Gibbs weights* or *partial costs* $g_{i\nu}$ are formally defined as the costs $\mathcal{H}(\mathbf{M}^{i \leftarrow \nu})$ for a given assignment matrix $\mathbf{M}$. Here $\mathbf{M}^{i \leftarrow \nu}$ denotes the configuration, which is obtained by replacing the old prototype of image site i with the new prototype ν.
- Assign the image site to the class label which produces minimal costs. Formally,

$$M_{i\alpha} = 1 \quad \text{iff } \alpha = \arg\min_{\nu} g_{i\nu} \tag{11}$$

Note, that to compute the minimal $g_{i\nu}$ in (11) we may add or subtract any part of the cost function not depending on i,

e.g. $g_{i\nu} = \mathcal{H}(\mathbf{M}^{i\leftarrow\nu}) - \mathcal{H}(\mathbf{M}^{i\leftarrow 0})$, where $\mathcal{H}(\mathbf{M}^{i\leftarrow 0})$ is obtained from $\mathbf{M}$ by replacing $M_{i\nu}$ by 0 for all ν. The partial costs $g_{i\nu}$ are then equivalent to

$$g_{i\nu} = \mathbf{y}_\nu^t (\mathbf{p}_i + \mathbf{b}_{ii} \circ \mathbf{y}_\nu) \tag{12}$$

with the bookkeeping entities

$$\mathbf{p}_i = 2 \sum_{j\in\tilde{N}_i, j\neq i} b_{ij} \circ \sum_{\alpha=1}^{K} M_{j\alpha}\mathbf{y}_\alpha + \mathbf{a}_i \tag{13}$$

The bookkeeping scheme enables fast evaluation of the cost function. The bookkeeping entities have only to be updated locally when changing a site, i. e. only parts of the cost function are influenced by a change of the assignment variables $M_{i\nu}$. Further acceleration is gained by exploiting the fact that the assignment of a site can only change, if a neighboring site has already been changed since the last site visit. In an efficient implementation this is achieved by an adaptive site visitation schedule organized as a queue leading to acceleration factors of approximately four.

Algorithm I

```
INPUT w_ij, x_i
INITIALIZE M^{l_max} randomly
COMPUTE a_I^l, b_IJ^l according to (9) and (22).
FOR l = l_max, ..., 0
  IF (l ≠ l_max) PROPAGATE M_Iν^{l+1} to M_iν^l
  WHILE (K < K_max^l)
    SPLIT cluster with highest distortion
    REPEAT
      FOR i = 1,...,N^l: Insert i in QUEUE
      WHILE QUEUE not empty   // ICM loop
        SET i = next element of QUEUE
        COMPUTE g_iν according to (12)
        UPDATE M_iν^l according to (11)
        IF M_iν^l changed
          FOR ALL j ∈ Ñ_i^l:
            INSERT j in QUEUE
            UPDATE p_j
      UPDATE Y according to (17)
    UNTIL converged
END
```

3.2. Computing a new color palette

For fixed Boolean variables $\mathbf{M}$ the optimization of $\mathcal{H}(\mathbf{M},\mathbf{Y}) = \mathcal{H}(\mathbf{Y})$ yields a simple matrix equation. Let $\mathbf{S} = (\mathbf{s}_{\nu\alpha}) \in \mathbb{R}^{K\times K\times 3}$ and $\mathbf{R} = (\mathbf{r}_\nu^t) \in \mathbb{R}^{K\times 3}$, where

$$\mathbf{s}_{\nu\alpha} = \sum_{i=1}^{N} \sum_{j\in\tilde{N}_i} M_{i\nu} M_{j\alpha} \mathbf{b}_{ij} \tag{14}$$

$$\mathbf{r}_\nu = \sum_{i=1}^{N} M_{i\nu} \mathbf{a}_i \tag{15}$$

then the dithered clustering cost function can be rewritten as the quadratic form

$$\begin{aligned}\mathcal{H}(\mathbf{Y}) &= \sum_{\nu=1}^{K}\sum_{\alpha=1}^{K} \mathbf{y}_\alpha^t (\mathbf{s}_{\nu\alpha} \circ \mathbf{y}_\nu) + \sum_{\nu=1}^{K} \mathbf{r}_\nu^t \mathbf{y}_\nu \\ &= \sum_{k=1}^{3} \left(\sum_{\nu=1}^{K}\sum_{\alpha=1}^{K} s_{\nu\alpha k} y_{\nu k}^t y_{\alpha k} + \sum_{\nu=1}^{K} r_{\nu k}^t y_{\nu k} \right)\end{aligned} \tag{16}$$

Note that the color dimensions decouple. Denote by $\mathbf{S}_k = (\mathbf{s}_{\nu\alpha})_k \in \mathbb{R}^{K\times K}$ the matrix spanned by color plane k and by $\mathbf{Y}_k \in \mathbb{R}^K$ and $\mathbf{R}_k$ the respective column vectors corresponding to color plane k. Setting the derivatives $\partial\mathcal{H}/\partial y_{\alpha k} = 0$ the optimal $\mathbf{Y}$ is now given column wise (color wise) by

$$\mathbf{Y}_k = -(2\mathbf{S}_k)^{-1}\mathbf{R}_k \tag{17}$$

It is straight forward to prove that the overall alternating minimization scheme converges to a local minimum of (5)[27].

3.3. Multiscale Optimization

The statistics of natural images support the assumption that colors are distributed homogeneously in images, i.e. pixels adjacent to each other contain with high probability similar colors. This fact can be exploited to significantly accelerate the optimization process by minimizing the criterion over a suitable nested sequence of subspaces in a coarse to fine manner. Each of these subspaces is spanned by a greatly reduced number of optimization variables. In contrast to most multiresolution optimization schemes the identical cost function is optimized at all grids, solely the variable configuration space is reduced.

This strategy is formalized by the concept of *multiscale optimization*[20] and it leads in essence to cost functions redefined on a coarsened version of the original image. Formally, we denote by $\mathcal{S}^0 = \mathcal{S}$ the original set of sites and we assume that a set of grid sites $\mathcal{S}^l = \{1,\ldots,N^l\}$ is given for each coarse grid level l. Throughout this section coarse/fine grid entities are denoted by upper/lower case letters. Define a coarsening map C_l on the sets of indices:

$$C_l : \mathcal{S}^l \to \mathcal{S}^{l+1}, \qquad i \mapsto I = C_l(i) \tag{18}$$

where each fine grid point is linked to a single coarse grid point. Typically $\mathcal{S}^0 = \mathcal{S}$ corresponds to the set of pixel sites and $\mathcal{S}^{l+1}$ is obtained by subsampling $\mathcal{S}^l$ by a factor of 2 in each direction, i.e. 4 sites are combined into a single coarse site by the two–dimensional index operation $(I,J) = (\lfloor i/2 \rfloor, \lfloor j/2 \rfloor)$. Since this operation is a many-to-one map the inverse C_l^{-1} is a subset of the fine grid sites, $C_l^{-1}(I) \subset \mathcal{S}_l$. Multiscale optimization proceeds not by coarsening the image, but by *coarsening the variable space*. Each coarse grid is associated with a reduced set of optimization variables $\mathbf{M}^l \in \mathcal{M}^l$,

$$\mathcal{M}^l = \left\{ \left(M_{I\nu}^l\right)_{\substack{I=1,\ldots,N^l \\ \nu=1,\ldots,K}} : M_{I\nu}^l \in \{0,1\} \right\} \tag{19}$$

Thus K Boolean variables $M_{I\nu}^l$ are attached to each grid point I denoting whether the set of respective pixels is assigned to

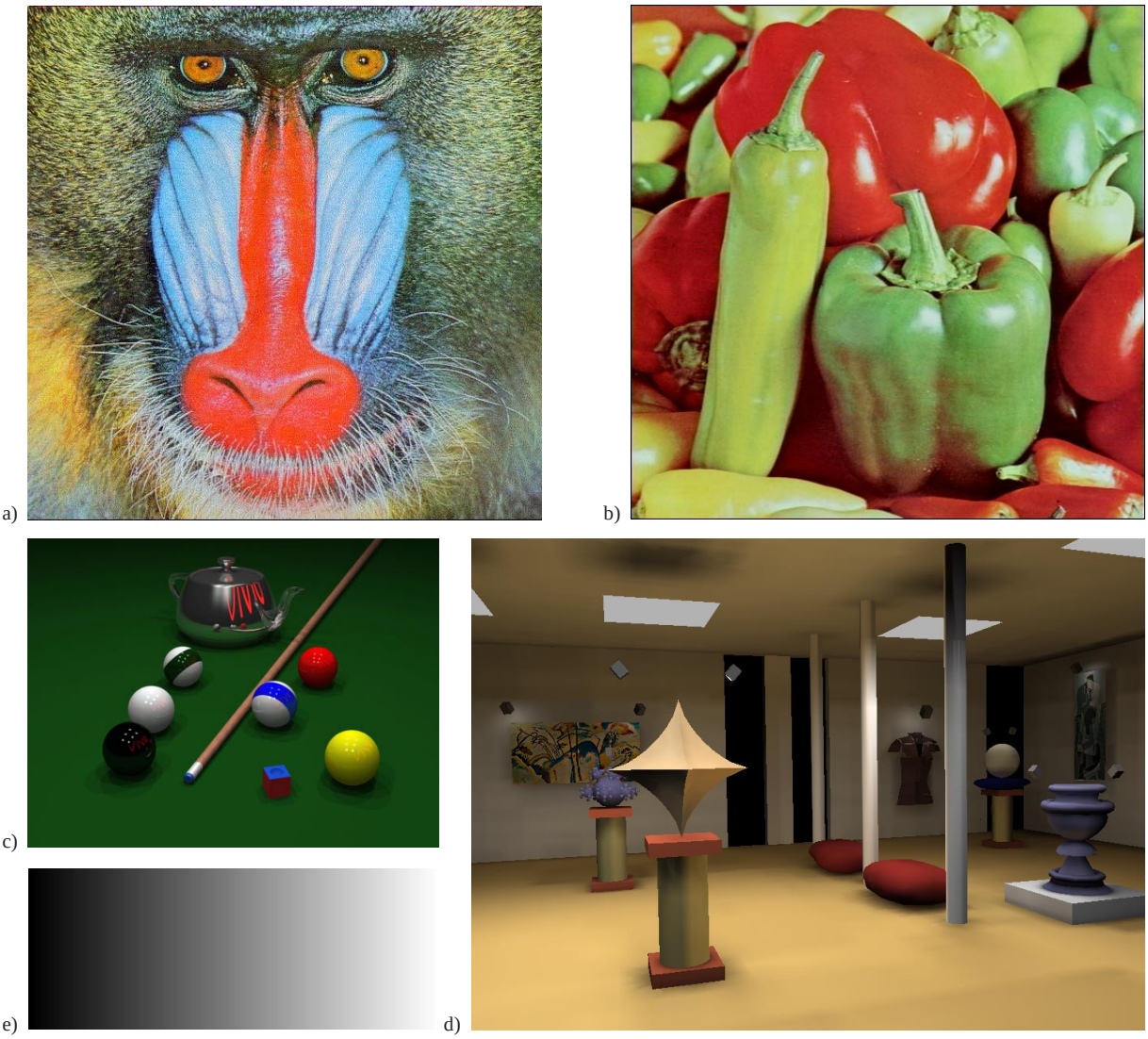

Figure 2: *Original images used for the different experiments: (a) "Mandrill" (171.877 colors), (b) "Peppers" (111.344 colors), (c) "Pool" (13.604 colors), (d) "Museum" (31.812 colors), and (e) Grey wedge (256 colors).*

color $\mathbf{y}_\nu$. Coarsened cost functions at level $l+1$ are defined by proper restriction of the optimization space at level l:

$$\mathcal{H}^{l+1}(\mathbf{M}^{l+1} \in \mathcal{M}^{l+1}, \mathbf{Y}) := \mathcal{H}^l(\mathbf{M}^l \in \tilde{\mathcal{M}}^l : M^l_{i\nu} = M^{l+1}_{C_l(i)\nu}, \mathbf{Y})$$

where

$$\tilde{\mathcal{M}}^l = \left\{ \mathbf{M}^l \in \mathcal{M}^l : M^l_{i\nu} = M^l_{j\nu} \text{ for } C_l(i) = C_l(j) \right\} \quad (20)$$

denotes the subspace $\tilde{\mathcal{M}}^l \subset \mathcal{M}^l$ with identical assignments for sites with the same coarse grid point. Now introduce a coarse grid neighborhood by

$$\tilde{N}^{l+1}_I = \left\{ J \,\middle|\, \exists i \in C_l^{-1}(I), j \in C_l^{-1}(J) : j \in \tilde{N}^l_i \right\} \quad (21)$$

We recursively define

$$\mathbf{b}^{l+1}_{IJ} = \sum_{\substack{i \in C_l^{-1}(I)\ j \in C_l^{-1}(J) \\ \wedge\ j \in \tilde{N}_i}} \mathbf{b}^l_{ij}, \qquad \mathbf{a}^{l+1}_I = \sum_{i \in C_l^{-1}(I)} \mathbf{a}^l_i \quad (22)$$

For the dithered quantization cost function (5) the following coarse grid cost functions are obtained:

$$\begin{aligned} \mathcal{H}^l(\mathbf{M}^l, \mathbf{Y}) \;=\; & \sum_{I=1}^{N^l} \sum_{J \in \tilde{N}^l_I} \sum_{\nu=1}^{K} \sum_{\alpha=1}^{K} M^l_{I\nu} M^l_{J\alpha} \mathbf{y}^t_\alpha \left(\mathbf{b}^l_{IJ} \circ \mathbf{y}_\nu \right) \\ & + \sum_{I=1}^{N^l} \sum_{\nu=1}^{K} M^l_{I\nu} \left(\mathbf{a}^l_I \right)^t \mathbf{y}_\nu \end{aligned} \quad (23)$$

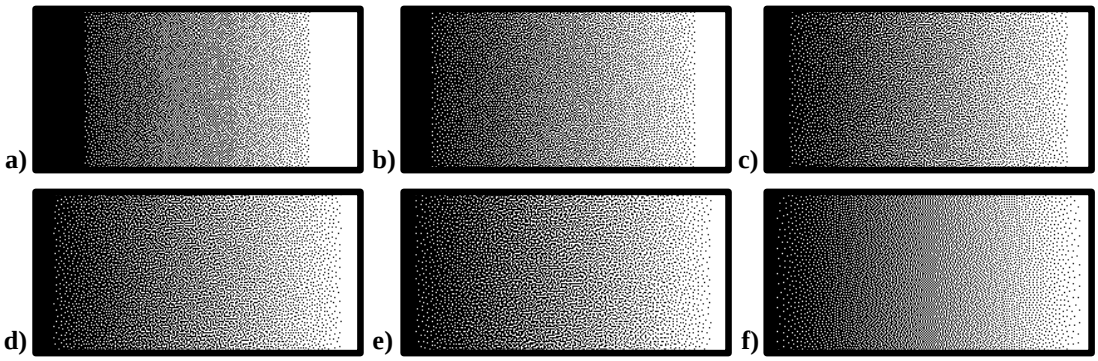

Figure 3: *Image quantization on a smooth transition of grey levels (256 different grey values): (a) to (e) dithered quantization with neighborhood sizes from* 3×3 *to* 11×11 *(from left to right), (f) Floyd–Steinberg (FS) dithering.*

Note, that $\mathcal{H}^l$ has the same functional form as $\mathcal{H}^0 = \mathcal{H}$ and, therefore, an optimization algorithm developed for $\mathcal{H}$ is applicable to any coarse grid cost function $\mathcal{H}^l$ without changes.

Algorithms like K–means or LBG[3] efficiently minimize $\mathcal{H}$ by *splitting techniques* to obtain successive solutions for a growing number of clusters. For ICM we adopt an idea from K–means clustering by splitting clusters with high distortion. Since the number of effective data points available does drastically reduce at coarser resolution levels, splitting strategy and coarse–to–fine optimization should be interleaved. After prolongation to level l the ICM optimization is continued at a finer resolution level using the obtained color palette as starting point for the optimization at this level. The question of choosing the maximal number of clusters for a given resolution has been addressed in a statistical learning theory context in[21]. We adopt this approach by choosing $K^l_{\max} \sim N^l / \log N^l$ and choosing the proportionality factor on an empirical basis. The complete algorithm is summarized in Algorithm I.

Figure 4: *Dithered image quantization using* 16 *colors in image "Museum" (neighborhood size* 3×3*).*

4. Results

To evaluate its quality the proposed dithered quantization algorithm is compared with several standard color reduction methods, which all employ both quantization and dithering. As *median-cut quantizer*[1] in conjunction with the Floyd–Steinberg dithering algorithm **ppmquant** found in the PPM tools by Jef Poskanzer is used. If the image contains a large number of different colors **ppmquant** employs a uniform quantization step in advance to decrease the histogram size and to improve performance. The implementation of **octree quantization**[2] is based on C code published in Dr. Dobbs Journal. We also compare our approach with the **self-organizing map** (SOM) inspired algorithm by Dekker[5]. As the simplest alternative we applied a **uniform quantization** (2:2:2) for 64 colors followed again by a Floyd–Steinberg dithering procedure for error distribution[8]. A representative set of images has been chosen for comparison and evaluation, which are depicted in Fig. 2.

To examine the dithering properties of the novel cost function independently from the built–in quantization several runs on an artificial image with smooth transition of grey values as depicted in Fig. 3 have been carried out. The role of the neighborhood size for the quality of our dithering approach is the main purpose of this experiment. Therefore the available two colors were fixed as black & white and only the assignments of pixels to the given color values were optimized. Fig. 4 gives an example of a radiosity image "Museum" reduced to 16 colors.

It has to be noticed (Fig. 3) that the (subjective) dithering quality grows with neighborhood size. Starting with a neighborhood size of 5×5 a smooth transition between grey values is obtained, while the smaller neighborhood of 3×3 suffers from its limited variability to distribute black and white pixels and generates artificial 'edge' structures. In contrast,

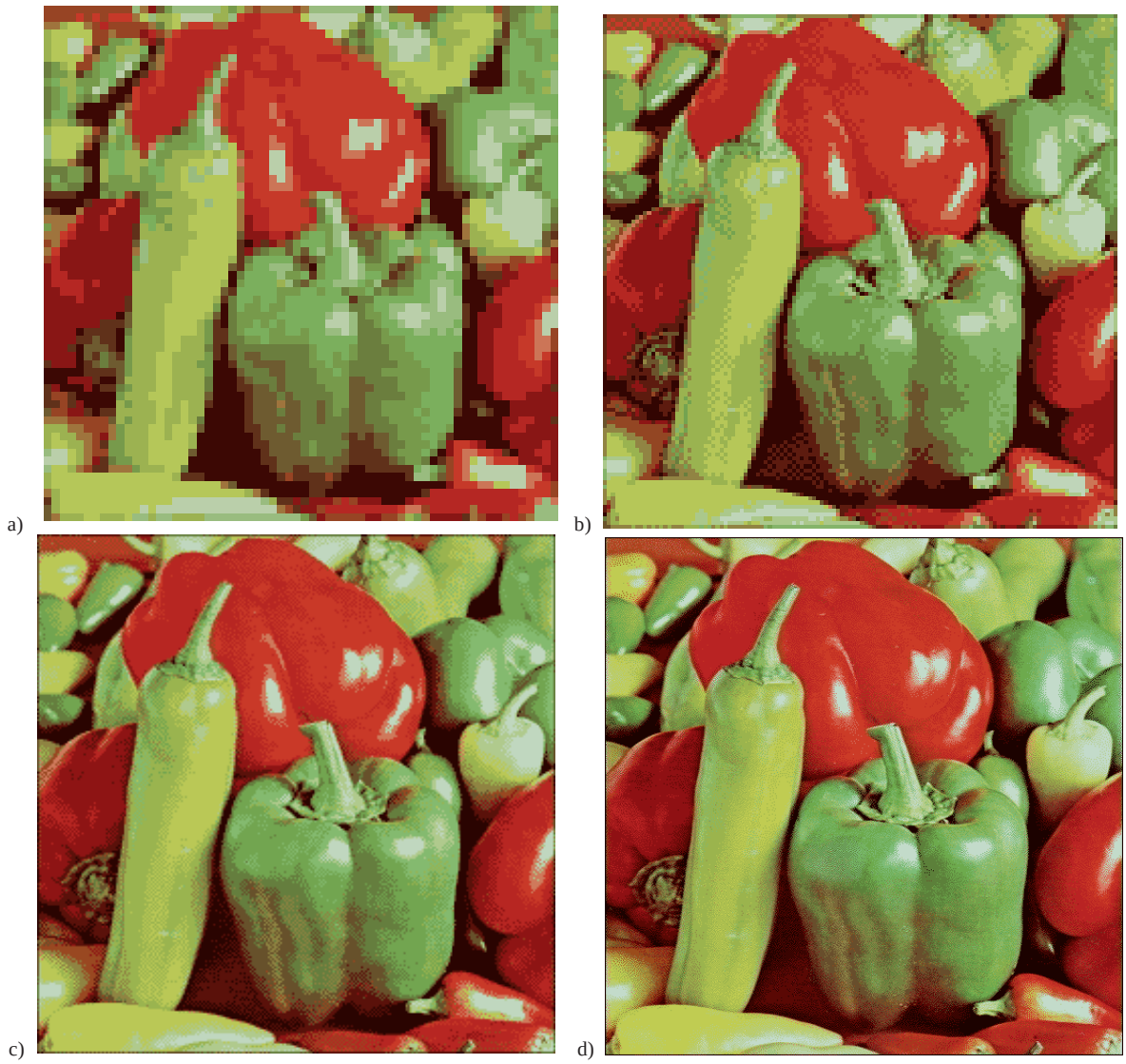

Figure 6: *Multiscale optimization of the "Peppers" image. (a) to (c) intermediate coarse scale results (d) resulting quantized image. All images with 16 colors. The neighborhood size has been set to* 5×5.

the Floyd–Steinberg algorithm introduces significant visual distortions by edge effects and over–regular patterns and it is not capable to generate a smooth transition of grey values.

As already indicated by Bouman et al.[12] the conjunction of quantization and dithering should yield distortions with small contributions in the low spatial frequencies, as high frequency components of the error signal are less visible to the human observer. Fig. (5) outlines that the dithered quantization approach in fact reduces the low frequency components of the error signal, by raising the overall distortion error and the high frequency parts. We present only the spectrum of the error in the luminance, whereas the picture is the same in the chromatic color planes. For larger neighborhood sizes the changes in the error spectrum are similar to the depicted 5×5 neighborhood result.

The top two rows of Fig. 8 compare the full dithered quantization approach to median cut / Floyd–Steinberg (FS) with respect to quality for different number of colors. The pool billiards image was selected for its large range of colors. Especially the billiard–balls represent smooth transitions from dark to bright primary colors. It can be seen that the proposed algorithm is able to distribute a small number of available colors in a more efficient way then FS. Notice especially the lack of any yellow color in the median cut quan-

a)  b) 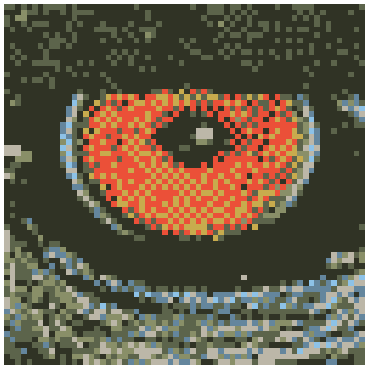 c) 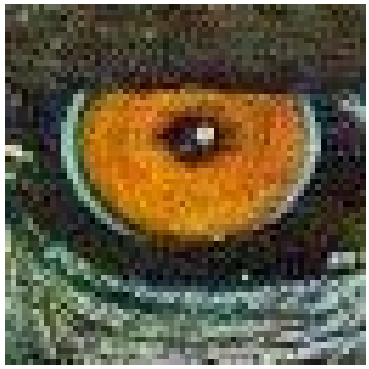

Figure 7: *Dithered quantization of the image "Mandrill": (a) Image reduced to 8 colors, (b) detail of 8 color image and (c) same sub image from the original image with 171.877 colors. The neighborhood size is* 3×3.

	Pool	Peppers	Mandrill	Museum
dithered quantization	0.35 (0.72) 36 s	1.34 (3.20) 81 s	1.82 (4.50) 116 s	0.57 (1.32) 131 s
SOM + FS	0.54 (0.95) 3 s	1.95 (3,53) 4 s	3.10 (5.12) 5 s	0.98 (1.7) 9 s
median cut + FS	1.43 (1,95) 1 s	2.03 (3.51) 2 s	2.49 (4.36) 3 s	0.95 (1.74) 4 s
octree + FS	1.49 (2.36) 8 s	3.59 (5.2) 11 s	6.33 (8.76) 9 s	1.38 (2.59) 16 s
uniform (2:2:2) + FS	6.69 (17.65) 2 s	7.03 (19.6) 3 s	6.84 (17.27) 3 s	7,14 (20.4) 4 s

Table 1: *Comparison of different color reduction methods for quantization to 64 colors. First row: Quality measured in terms of (5) on a scale* $[0,100]$ *(average deviation, i. e.* $\mathcal{H}(\mathbf{M},\mathbf{Y}) = \frac{100}{\sqrt{3}} \frac{1}{N} \sum_{i=1}^{N} \|\mathbf{c}_i(\mathbf{X}) - \mathbf{c}_i(\mathbf{MY})\|_2$*, where the distance between a complete black image and a white image (maximal distance) is given by* $\sqrt{3}$*, i. e. the diagonal of a unit cube representing the color space). In brackets the quality measured by pixel wise squared difference (K–means criterion) is given. Second row: run–time in seconds measured on a Pentium Pro 200. All quantizations are performed in the RGB color space. The neighborhood size for the dithered clustering approach has been set to* 3×3.

tized image. The reason for this unsatisfactory behavior is due to the size of the green area in the original image as the median cut quantizer assigns too much resources, i. e. color prototypes, to the green color values. This deficit is fundamentally caused by the fact that median cut creates clusters with approximately equal size, i. e. attributed distortion error, instead of rigorously optimizing a distortion measure. Depending on the number of desired colors only four to one prototypes are left for all other colors in the image. To represent the large range of remaining colors the center color with its greyish appearance was taken. In Fig. 8 also the result for other standard color reduction approaches are depicted, where the dithered quantization approach always visually outperforms the other algorithms. It becomes apparent, that especially for small color tables the other approaches are not able to provide the correct colors for the color reduction problem. This is a clear indication for the superiority of the locally defined dithered quantization cost function.

In Fig. 7 the "Mandrill" image quantized to 8 colors is depicted. It is possible to reduce the number of colors from 171.877 with only minor perceptive defects, as many illusionary colors are created by dithering. This is illustrated by magnification of the monkey's eye in Fig. 7 (b) and (c), which demonstrates that very different colors can be used to create a highly similar visual perception.

The quality and performance results for all images are summarized in Table 1. In absence of a better psychophysically defined distortion measure the quality according to the *K*–means criterion and the novel dithered quantization cost

Figure 8: *Comparison of different image quantization algorithms (from left to right: 256, 64, 16 and 8 colors): (a) Dithered Quantization (*3×3 *neighborhood) (b) Median-Cut + FS (c) Octree + FS (d) SOM–Algorithm + FS (e) Uniform Quantizer + FS.*

function (5) are reported, although we are convinced that (5) better reflects visual distortion. As expected, according to its own cost function dithered quantization outperforms all other methods by an order of magnitude. But even according to the K–means criterion it produces better results, which can be explained by the fact that the heuristic dithering procedures tend to increase the K–means distortions costs drastically.

On the other hand it has to be stressed that the computational complexity of dithered quantization increases significantly in comparison to the other methods, see again Table 1. Thus, the design of efficient optimization algorithms like multiscale methods turns out to be indispensable. As seen in Table 2 multiscale optimization accelerates the optimization by a factor 2–5. Fig. 6 illustrates the typical progress in multiscale optimization. According to (22), colors are replaced by local averaging in coarse images, with coarse grid colors corresponding to perceived colors. At the same time the neighborhood smoothing kernel sharpens according to (22). Consequently, dithered optimization on coarser grids has a tendency to suppress dithering of colors thereby introducing a bias towards local minima with homogeneous colors.

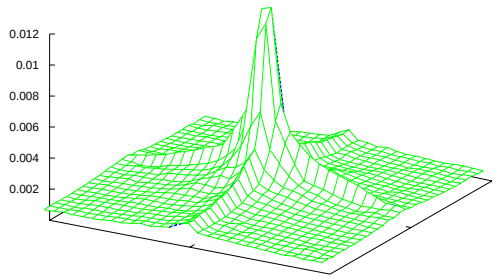

a)

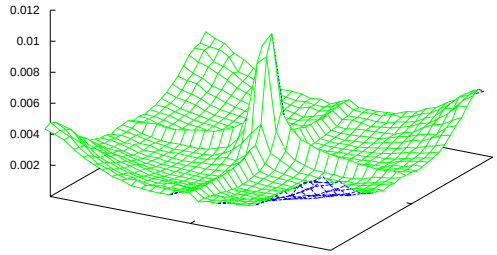

b)

Figure 5: *Spatial spectra of the quantization error for the image "Peppers" reduced to 16 colors. Each plot corresponds to the Fourier transformation of the deviation in the luminance component. a) K–means spectrum and b) dithered quantization spectrum (*5×5 *gaussian kernel).*

	Multiscale		Single scale	
Pool	0.66	111 s	2.43	323 s
Peppers	1.92	189 s	2.22	501 s
Mandrill	2.34	221 s	3.18	426 s
Museum	1.03	646 s	1.55	1694 s

Table 2: *Comparison of multiscale and single scale methods. First column: Quality measured in terms of (5). Second column: run–time in seconds measured on a PentiumPro 200. The images were quantized to 16 colors with a neighborhood size of* 7×7.

On the other hand it is well known that multiscale coarsening causes *implicit smoothing* of the energy landscape[20] and, therefore, avoids poor local minima. This effect is confirmed by the quality results in Table 2.

Our experiments also indicate that color reduction down to less than 10 colors still results in recognizable images, which might be of interest for generating iconized images in multimedia applications. Also, some widespread operating systems restrict icons to resolutions of 32×32 with a maximum of 12 colors. Another application of this low color reduction might be the automatic generation of so–called thumbnails for image databases. For a comparison of our approach with the SOM approach for this specific application see Fig. 9.

5. Conclusion

We have presented a novel approach to simultaneous color image quantization and dithering by introducing a novel quality measure and by employing advanced concepts from the field of discrete optimization. The new optimization criterion incorporates dithering in the clustering cost function based on a model of the human visual system. An efficient ICM algorithm has been developed and an extension to multiscale optimization has been derived to accelerate the algorithm.

It has been demonstrated that the algorithm yields a significant improvement in quality compared to alternative approaches on a large set of images. The results are especially convincing for small color palettes, where standard quantization schemes completely fail. Furthermore we use our appraoch for the color reduction of a series of icons indicating that one possible application might be the automatic design of color reduced icons for multimedia tools. Moreover, it is possible to incorporate a (partially) predefined color palette in the optimization process.

In the experiments the generic dithered quantization cost function has been used in conjunction with a very simple model of human perception. Future research will examine more elaborated models with emphasis on color constancy and preservation of features like edges. In addition, extensions of the implemented algorithm to image sequences seems straightforward from both the modeling and the algorithmic perspective.

References

1. P. Heckbert, "Color image quantization for frame buffer displays," *Computer Graphics*, vol. 16, no. 3, pp. 297–307, 1982.
2. M. Gervauz and W. Purgathofer, "A simple method for color quantization: Octree quantization," in *Graphic Gems*, pp. 287–293, Academic Press, New York, 1990.
3. Y. Linde, A. Buzo, and R. Gray, "An algorithm for vector quantizer design," *IEEE Transactions on Communications*, vol. 28, no. 1, pp. 84–95, 1980.

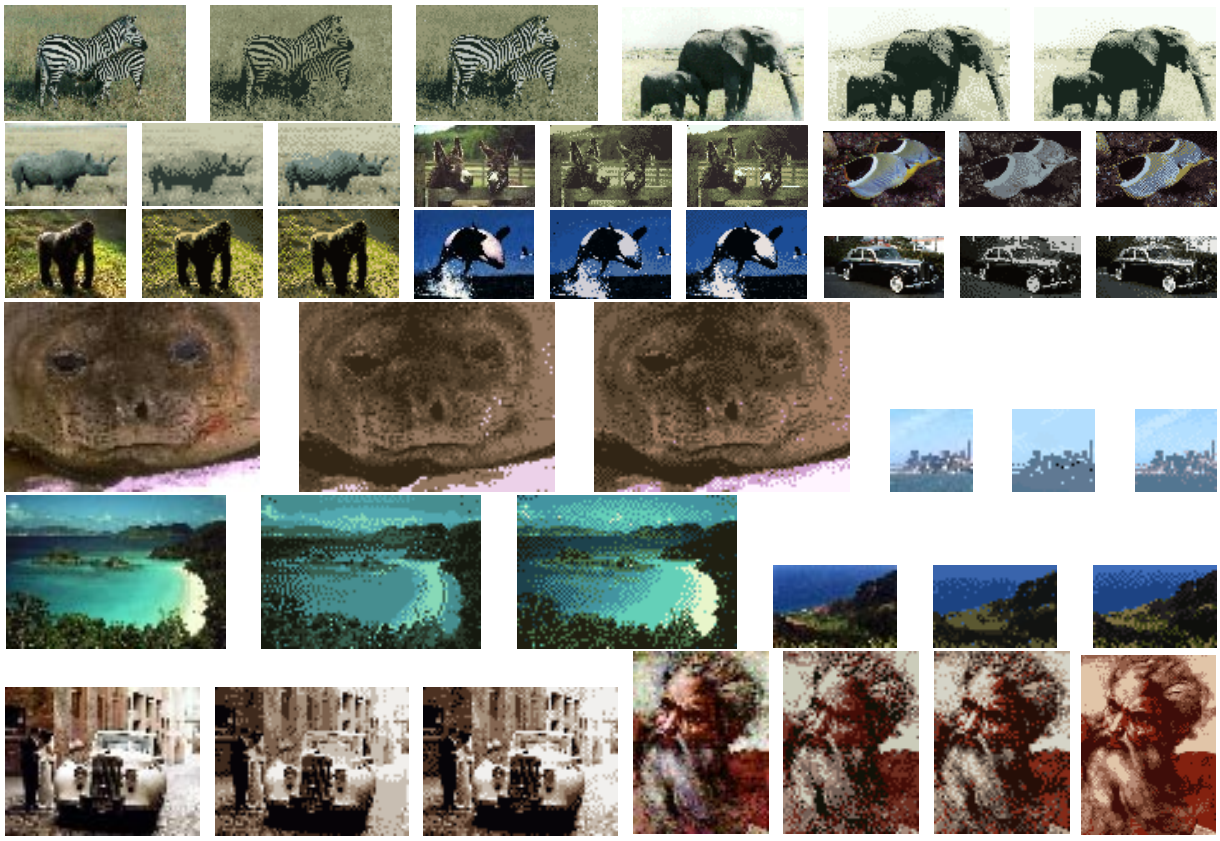

Figure 9: *Comparison of the dithered quantization approach with the SOM approach, where each image is subsampled to smaller size and reduced to 6 colors. Left: Subsampled Image. Middle: SOM approach with FS. Right: dithered quantization (neighborhood size* 3×3*). For each of these images it takes less than 1s for both schemes to perform the color reduction. Note, that for the last icon also the corresponding intermediate result of the multiscale optimization is depicted, indicating that this also might be a promising approach for the automatic generation of iconized images* [27].

4. G. Braudaway, "A procedure for optimum choice of a small number of colors from a large palette for color imaging," in *Electron Imaging'87*, 1987.

5. A. Dekker, "Kohonen neural networks for optimal colour quantization," *Network: Computation in Neural Systems*, vol. 5, pp. 351–367, 1994.

6. A. Jain and R. Dubes, *Algorithms for Clustering Data*. Prentice Hall, 1988.

7. R. Ulichney, *Digital Halftoning*. MIT Press, 1987.

8. R. Floyd and L. Steinberg, "An adaptive algorithm for spatial greyscale," in *Proc. SID, Vol. 17, No. 2*, Wiley, 1976.

9. T. Flohr, B. Kolpatzik, R. Balasubramanian, D. Carrara, C. Bouman, and J. Allebach, "Model based color image quantization," in *Proceedings of the SPIE: Human Vision, Visual Processing, and Digital Display IV* (J. Allebach and B. Rogowitz, eds.), vol. 1913, pp. 265–270, 1993.

10. J. Sullivan, R. Miller, and G. Pios, "Image halftoning using a visual model in error diffusion," *Journal of the Optical Society of America A*, vol. 10, pp. 1714–1724, 1993.

11. T. Pappas, "Model–based halftoning of color images," *IEEE Transactions on Image Processing*, vol. 6, no. 7, pp. 1014–1024, 1997.

12. M. Orchard and C. Boumann, "Color quantization of images," *IEEE Transactions on Signal Processing*, vol. 39, pp. 2677–2690, 1991.

13. X. Wu, "Color quantization by dynamic programming and principal analysis," *ACM Transactions on Graphics*, vol. 11, no. 4, pp. 384–372, 1992.

14. L. Akarun, D. Özdemir, and Ö. Yalcun, "Joint quantization and dithering of color images," in *Proceedings*

of the International Conference on Image Processing (ICIP'96), pp. 557–560, 1996.

15. P. Scheunders and S. D. Backer, "Joint quantization and error diffusion of color images using competitive learning," in *IEEE International Conference on Image Processing (ICIP)*, pp. 811–814, 1997.
16. F. Campbell, "The human eye as an optical filter," *Proceedings of the IEEE*, vol. 56, no. 6, pp. 1009–1014, 1968.
17. J. Mannos and D. Sakrison, "The effects of a visual fidelity criterion on the encoding of images," *IEEE Transactions on Information Theory*, vol. 20, no. 4, pp. 525–536, 1974.
18. R. Näsänen, "Visibility of halftone dot textures," *IEEE Transactions on Systems, Man and Cybernetics*, vol. 14, no. 6, pp. 920–924, 1984.
19. K. Mullen, "The contrast sensitivity of human color vision to red–green and blue–yellow chromatic gratings," *Journal of Physiology*, vol. 359, pp. 381–400, 1985.
20. F. Heitz, P. Perez, and P. Bouthemy, "Multiscale minimization of global energy functions in some visual recovery problems," *CVGIP: Image Understanding*, vol. 59, no. 1, pp. 125–134, 1994.
21. J. Puzicha and J. Buhmann, "Multiscale annealing for real–time unsupervised texture segmentation," Tech. Rep. IAI–97–4, Institut für Informatik III (a short version appeared in: Proc. ICCV'98, pp. 267–273), 1997.
22. C. I. de L'Eclairage, "Colorimetry." CIE Pub. 15.2 2nd ed., 1986.
23. D. Alman, "Industrial color difference evaluation," *Color Res. Appl. 18 137-139*, 1993.
24. E. Kandel, J. Schwartz, and T. Jessel, *Principles of Neural Science*. Appleton & Lange, 3rd ed., 1991.
25. C. Atkins, T. Flohr, D. Hilgenberg, C. Bouman, and J. Allebach, "Model–based color image sequence quantization," in *Proceedings of the SPIE Conference on Human Vision, Visual Processing, and Digital Display V,*, vol. 2179, pp. 310–317, 1994.
26. J. Ketterer, J. Puzicha, M. Held, M. Fischer, J. M. Buhmann, and D. Fellner, "On spatial quantization of color images," in *Proceedings of the European Conference on Computer Vision*, 1998.
27. J. Puzicha, M. Held, J. Ketterer, J. Buhmann, and D. Fellner, "On spatial quantization of color images," Tech. Rep. IAI-TR-98-1, Department of Computer Science III / University of Bonn, 1998.